Thermomechanical analysis of the laminated object manufacturing (LOM) process

Fazil O. Sonmez and H. Thomas Hahn

The authors

Fazil O. Sonmez is based at the Department of Mechanical Engineering, Bogazici University, Bebek, Istanbul, Turkey.

H. Thomas Hahn is based at the Mechanical, Aerospace and Nuclear Engineering Department, University of California, Los Angeles, California, USA.

Abstract

LOM is one of the techniques for rapid prototyping, which is used to build three-dimensional solid objects. In this paper, a numerical analysis of the thermomechanical behavior of a laminate during the LOM process is presented. Models were developed to describe heat transfer and deformation phenomena. These models are incorporated into computer codes to generate numerical results. The numerical results show how the process parameters (e.g. roller temperature, velocity, indentation) are related to temperature and stress distributions within the laminate. By using this code, process conditions which are favorable to bonding are identified.

Rapid Prototyping Journal
Volume 4 · Number 1 · 1998 · pp. 26–36
 · ISSN 1355-2546

Introduction

Additive rapid prototyping is a new class of automated fabrication process in which a three-dimensional object is built directly from a surface or solid CAD file by electronically sectioning the designed object and constructing each cross section from the bottom up one layer at a time. The general purpose of rapid prototyping is to reduce the product development times by shortening the time between design and testing. With rapid development of this technology, one can easily envision that the traditional labor intensive and time consuming model building process will soon be superseded.

Laminated object manufacturing (LOM) is one of the most promising rapid prototyping techniques in terms of dimensional accuracy, speed and cost effectiveness. Paper coated on one side with a thermoplastic adhesive is a commonly used material, resulting in wood-like structures.

The process is described in Figure 1. A sheet is laminated to previously laid and bonded layers by a hot roller. After the new layer is bonded, a focused laser beam incises the outline of the part. Laser power is adjusted to cut through only one layer of lamination. The unused material is left in place, however, diced with cross-hatches for easy removal. Layer by layer the part is built (Figure 2). Once all layers have been laminated and cut, excess material is removed to expose the finished part (Chua, 1994; Feygin *et al.*, 1992; Kochan, 1994; Muraski, 1990; Wood, 1993).

Despite the advantages of the LOM process, some problems are yet to be overcome. The major difficulties encountered in the current LOM practice are the operation with less than the optimum processing parameters and inability to maintain uniform processing conditions throughout the lamination process. Process parameters are found by trial and error. Due to the large number of variables, this method rarely yields optimum parameters, resulting in undesirably low processing speeds. As the worst case, weak interlaminar bonds and delaminations in

This article is based on the work supported by the Office of Naval Research Grant N00014-92-J-1846 with Dr Tapa D.S. Rajapakse as the program director. The authors are also thankful for the data received from Helisys Inc.

Rapid Prototyping Journal
Volume 4 · Number 1 · 1998 · 26–36

Figure 1 Formation of a new layer

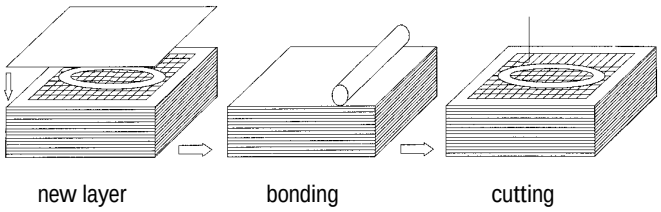

Figure 2 Cross-section of the part

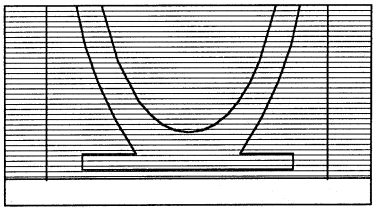

finished parts may occur. In addition, excessive heat and pressure may cause material degradation. As the thickness of the laminate increases, process parameters should be modified in order to maintain uniform temperature and stress states. However, in the current practice, these parameters are kept constant or manually changed through the manufacturing process. Nonuniform process conditions usually lead to warpage and distortions in the final product. Sometimes, the distortion is severe enough to reject the part.

Achieving high dimensional accuracy and improving productivity together with part quality require a comprehensive understanding and close control of the effects of process parameters (e.g. roller velocity, temperature, indentation). As in other lamination techniques for polymers, the thermomechanical history that a part experiences determines the quality of bonding. Except for some empirical equations (Pak and Nisnevich, 1994), there are no studies in the literature that relate process parameters to the stress and temperature states within the laminate.

In this paper, modeling of thermomechanical behavior during the LOM process is proposed. Based on the finite element method, heat transfer and stress analyses are carried out. The stress analysis problem is formulated as a quasi-steady state rolling contact problem. Coulombís dry friction law is used to describe the friction phenomenon between the roller and the laminate. Thermal expansion coefficients are allowed to be temperature dependent. In the heat transfer analysis, the temperature dependency of thermal conductivity and specific heat is taken into account. Length of the contact with the roller as calculated in the stress analysis is used in the heat transfer analysis. Therefore stress and heat transfer analyses are fully coupled.

Formulation of the problem

Heat transfer analysis

Figure 3 displays the control volume, the boundaries and the coordinate system used. The *y* axis passes from the nip point, where the sheet and the substrate merge, not the center of the roller. The mold is also included in the control volume.

Boundary conditions

Considering the forced convection to the air due to the ventilation system inside the chamber and the time elapsed during laser cutting, the temperature of the laminate and mold can be assumed to return to its steady-state value before a new layer is laid. Therefore, on the boundary S_1 in Figure 3, the temperature is constant and equal to the far field temperature, which is the temperature in the chamber:

$$T = T_c \text{ on } S_1 \quad (1)$$

Since the new layer is introduced from the outside of the chamber just before lamination, on S_2, the temperature of the freshly laid sheet is uniform and equal to the room temperature:

$$T = T_{room} \text{ on } S_2 \quad (2)$$

Considering that the roller is large and made of a highly conductive material, which is aluminum (210W/m°C) and the transverse heat conductivity of the paper laminate is very low (≈ 0.18W/m°C), the temperature of the roller can be assumed to be constant. Heat flux from the roller to the laminate can then be approximated by introducing an effective heat transfer coefficient, h_r ($Wm^{-2}°C^{-1}$). In

Figure 3 The part geometry and the control volume

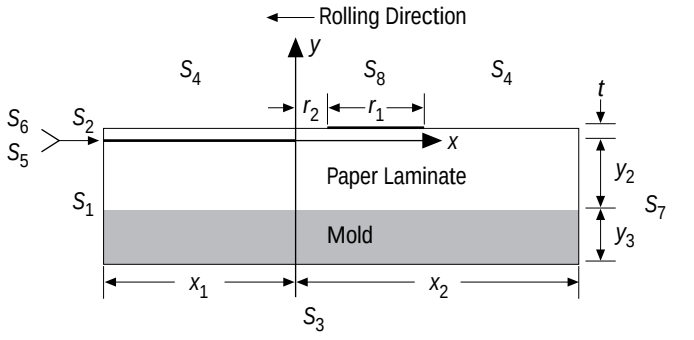

Rapid Prototyping Journal
Volume 4 · Number 1 · 1998 · 26–36

this case, the boundary between the laminate and the roller is treated as a convection boundary condition. We have thus the following convection boundary condition across the contact area:

$$k_T \frac{\partial T}{\partial y} = -h_r (T - T_r) \qquad \text{on } S_8 \tag{3}$$

where k_T the transverse conductivity of the laminate and T_r is the roller temperature. The top surface except the area in contact with the roller is exposed to air. We then have the following convection boundary condition on S_4:

$$k_T \frac{\partial T}{\partial y} = -h_a (T - T_a) \qquad \text{on } S_4 \tag{4}$$

where T_a is the temperature of the air inside the chamber. The bottom surface (S_3) is exposed to still air. The same relation in equation 4 holds. However, the heat transfer coefficient is different and the room temperature is used as the ambient temperature.

The air trapped between the freshly laid sheet and the laminate serves as an insulator up to the nip point. Therefore, there is no heat transfer on the boundaries S_5 and S_6.

$$\frac{\partial T}{\partial y} = 0 \qquad \text{on } S_5 \text{ and } S_6 \tag{5}$$

The control volume is taken to be so long that the dominant heat transfer mode at the right edge is heat transport due to the motion of the control volume rather than heat conduction. On the right hand side of the control volume, the temperature gradient is taken to be zero:

$$\frac{\partial T}{\partial x} = 0 \qquad \text{on } S_7 \tag{6}$$

Governing equation

Several assumptions have been made to simplify the analysis. In comparison to the amount of heat supplied to the material, mechanical heating through deformation is negligible.

Even though the laminate is heterogeneous with the paper and the adhesive, having different thermophysical properties, in the analysis it is treated as an anisotropic but homogeneous continuum. Also laser cuts are assumed to have negligible effect on heat conduction.

The material is uniformly heated though the width and heat losses through the edges are negligible, so that the heat conduction problem can be reduced to a two-dimensional analysis. It should be noted that uniform heating through the width is essential for uniform bonding and minimum residual stresses. Although temperature gradients may exist very close to the edges, considering that material near the edges is discarded after the process is finished, we do not need to account for these effects.

A quasi-steady state is assumed to prevail throughout the process. Namely, process conditions do not change with respect to the roller. Considering that the laser cuts are small, their existence is assumed not to disturb the steady state condition. Previous studies for similar processes (Sonmez and Han, 1995; forthcoming a) showed that, because of local heating, even a very small control volume could be used for analysis to give sufficiently accurate results. Nevertheless, dimensions of this control volume will be chosen so as to render the quasi-steady state assumption valid.

When the coordinates are fixed to the roller and the process conditions do not change with respect to this coordinate system, the governing equation for energy balance in the Eulerian control volume becomes (Brodkey and Hershey, 1988):

$$k_L \frac{\partial^2 T}{\partial x^2} + k_T \frac{\partial^2 T}{\partial y^2} = \rho C_p v_x \frac{\partial T}{\partial x} \tag{7}$$

where k_L and k_T are the longitudinal and transverse conductivities (W/m°C), respectively, v_x is the velocity of the roller (m/s), ρ is the density (kg/m^3) and C_p is the specific heat (J/kg°C).

Solution

Figure 4 shows the mesh structure, in which nonuniform rectangular elements are used. Using Galerkin's method, finite element formulation of equation 7 yields (Sonmez and Hahn 1995; forthcoming a):

$$\{T_u\} = [K_{uu}]^{-1} \left(\{P_u\} - [K_{us}] \{T_s\} \right) \tag{8}$$

where $\{T_u\}$ is the vector of unspecified node temperatures, $\{T_s\}$ is the vector of specified node temperatures. $[K_{uu}]$, $[K_{uu}]$, $\{P_u\}$ are parts of the global matrix and global force vector (Sonmez, 1995).

Given the boundary conditions and material properties, unknown node temperatures can be calculated from Equation 8. However, thermal conductivities k_L and k_T and specific heat C_p are functions of temperature. Consequently, $[K_{uu}]$, $[K_{us}]$, and $\{P_u\}$ will contain temperature dependent terms. In order to

Figure 4 Part of the mesh structure used in the analysis. Horizontal and vertical dimensions are not to scale

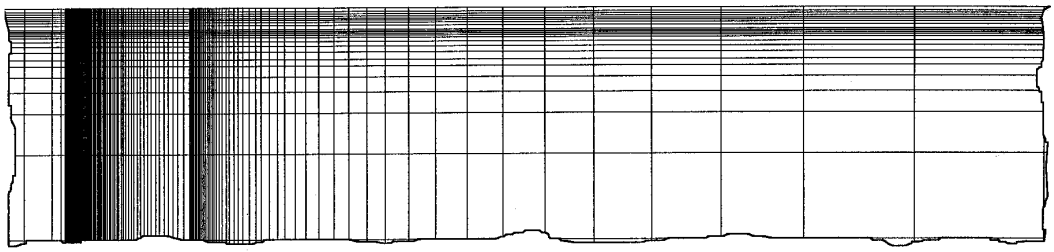

tackle this problem, an iterative solution procedure was followed. In the first iteration, average values of the temperature dependent material properties were used. In subsequent iterations, nodal temperatures obtained in the previous iteration were used to determine temperature dependent material properties.

The iterative process is continued until the maximum difference in temperature profiles obtained in two consecutive iterations becomes less than 1°C. After three or four iterations, the maximum difference usually satisfies this requirement. Convergence is checked at the nip point, the ends of the contact area, and where the maximum temperature occurs.

Stress analysis

Equilibrium equations

The roller moves with a constant velocity v_x, which is presumed to be sufficiently small so that all inertial effects are negligible. A steady state is assumed to apply within the Eulerian control volume moving with the roller away from the edges. Previous studies of rolling contact showed (Batra, 1977; Lynch, 1969) that the stress field was quite concentrated under the roller, and quickly decayed to zero as the distance from the roller increased. Experimental studies of LOM process (Sung Pak (nd)) also do not show any quality difference along the length of the laminate. It can then be concluded that process conditions along the path of the roller do not vary and the steady state assumption holds.

The width of the laminate is large, so that the plane strain assumption is valid. Neglecting the inertial forces, the equilibrium equations for two dimensional analysis become:

$$\frac{\partial \sigma_1}{\partial x} + \frac{\partial \sigma_6}{\partial y} = 0 \qquad \frac{\partial \sigma_6}{\partial x} + \frac{\partial \sigma_2}{\partial y} = 0 \tag{9}$$

Boundary conditions

The roller and the mold are assumed to be made of considerably harder material than the sheet material undergoing processing. Therefore, they are considered to be rigid.

The effect of friction is included in the stress analysis. Coulomb's friction law with a constant coefficient of friction is used. No differentiation is made between the adhesion, slip or partial slip phenomena.

On the top surface, we have the following boundary conditions:

$$\begin{aligned} &u_y(x,0) = d + \sqrt{R^2 - \left[x + u_x(x,0)\right]^2} - R && \rightarrow \text{in contact with the roller} \\ &F_s = F_r \mu \\ &\sigma_{ji} n_j = 0 && \rightarrow \text{not in contact with the roller} \end{aligned} \tag{10}$$

where d is the depth of indentation (Figure 5), R is the radius of the roller, u_x and u_y are the x and y components of the displacement, respectively, n_j is the outward directed unit normal to the surface, F_r and F_s are the normal and frictional forces, respectively and μ is the coefficient of friction at the contact surface. The first condition states that the deformed shape of the contact surface conforms to the circular shape of the rigid indentor, while the second condition comes from the Coulomb's friction law. The third condition indicates that, when the top surface is not in contact with the roller, it is not subject to any external force.

The bottom of the freshly laid paper and the top of the laminate up to the nip point are traction free.

$$\sigma_{ji} n_j = 0 \qquad y = t, \quad x < -\ell \tag{11}$$

The laminate is assumed to be perfectly bonded to the rigid mold. Therefore, at the bottom surface, the following boundary conditions are met:

$$\left.\begin{aligned} u_y &= 0 \\ u_x &= 0 \end{aligned}\right\} \qquad y = h \tag{12}$$

where h is the thickness of the laminate.

Rapid Prototyping Journal
Volume 4 · Number 1 · 1998 · 26–36

Figure 5 Configuration of the contact surface

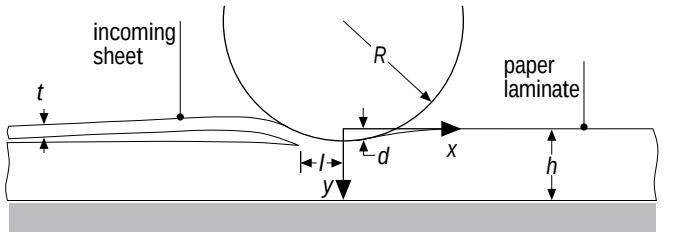

The control volume is sufficiently large so that the material entering or exiting from the control volume is stress free.

Normal stress on the contact surface is continuous, and hence it vanishes at the ends of the contact area.

Constitutive relations

In the analysis, linear elastic constitutive relations are used. Displacement gradients u_{ij} are in absolute value assumed to be much smaller than unity. Namely, the displacement changes slowly within the control volume. Displacement components u_i are also small with respect to the roller diameter when the coordinate axes are fixed to the roller. Besides, material nonlinearity is assumed to be negligible.

In plane strain, the displacements in the length and thickness directions (u_1 and u_2) depend only on x_1 and x_2, and the displacement in the width direction (u_3) is negligibly small:

$$u_1 = u_1(x_1,x_2)\ u_2 = u_2(x_1,x_2)\ u_3 = 0. \quad (13)$$

Consequently, all the strains related to the x_3 axis vanish:

$$\varepsilon_{13} = \varepsilon_{23} = \varepsilon_{33} = 0 \quad (14)$$

and the remaining displacements are related to the displacements by:

$$\varepsilon_{11} = u_{1,1}\ \varepsilon_{22} = u_{2,2}\ \varepsilon_{12} = \tfrac{1}{2}u_{1,2} + u_{2,1} \quad (15)$$

The laminate is transversely isotropic with its x_1-x_3 symmetry plane. The constitutive relations are then given by:

$$\begin{Bmatrix}\varepsilon_{11}\\ \varepsilon_{22}\\ \varepsilon_{33}\\ 2\varepsilon_{12}\end{Bmatrix} = \begin{bmatrix} \frac{1}{E_1} & -\frac{\nu_{12}}{E_2} & -\frac{\nu_{13}}{E_1} & 0 \\ -\frac{\nu_{21}}{E_1} & \frac{1}{E_2} & -\frac{\nu_{21}}{E_1} & 0 \\ -\frac{\nu_{13}}{E_1} & -\frac{\nu_{12}}{E_2} & \frac{1}{E_1} & 0 \\ 0 & 0 & 0 & \frac{1}{G_{12}} \end{bmatrix} \begin{Bmatrix}\sigma_{11}\\ \sigma_{22}\\ \sigma_{33}\\ \sigma_{12}\end{Bmatrix} + \begin{Bmatrix}\varepsilon^*_{11}\\ \varepsilon^*_{22}\\ \varepsilon^*_{33}\\ 0\end{Bmatrix} \quad (16)$$

where $\varepsilon^*_{ii}(t)$ are the thermal strains. Since the thermal expansion coefficients are temperature dependent, they are given by:

$$\varepsilon^*_{ii}(t) = \int_{T_o}^{T_f} \alpha_{ii}(T)\, dT \quad \text{(no sum on } i\text{)} \quad (17)$$

where T_0 is the base temperature. By setting $\varepsilon_{33} = 0$ in equation 16 and inverting, we obtain stress-strain relations as follows:

$$\begin{Bmatrix}\sigma_{11}\\ \sigma_{22}\\ \sigma_{12}\end{Bmatrix} = \begin{bmatrix} c_{11} & c_{12} & 0 \\ c_{12} & c_{22} & 0 \\ 0 & 0 & c_{66} \end{bmatrix} \begin{Bmatrix} \varepsilon_{11} - \left(\varepsilon^*_{11} + \nu_{13}\varepsilon^*_{33}\right) \\ \varepsilon_{22} - \left(\varepsilon^*_{22} + \nu_{21}\varepsilon^*_{33}\right) \\ 2\varepsilon_{12} \end{Bmatrix} \quad (18)$$

where:

$$\begin{aligned} c_{11} &= (1-\nu_{12}\nu_{21})DE_1 \\ c_{22} &= (1-\nu_{13}{}^2)DE_2 \\ c_{12} &= \nu_{12}(1+\nu_{13})DE_1 \\ c_{66} &= G_{12} \end{aligned} \quad (19)$$

here:

$$D = (1-2\nu_{12}\nu_{21}-\nu_{13}{}^2-2\nu_{12}\nu_{21}\nu_{13})^{-1} \quad (20)$$

Solution

Finite Element Method is used to solve the problem. The portion of the laminate to be analyzed is divided into eight-degrees-of-freedom rectangular elements concentrated at the interface as shown in Figure 6.

Using virtual work principle, the equilibrium equation is obtained as (Sonmez and Hahn, forthcoming b; Yang, 1986):

$$\{F\}=[K]\{\delta\}+\{H\} \quad (21)$$

Figure 6 Mesh structure used in the stress analysis. Horizontal and vertical dimensions are not to scale

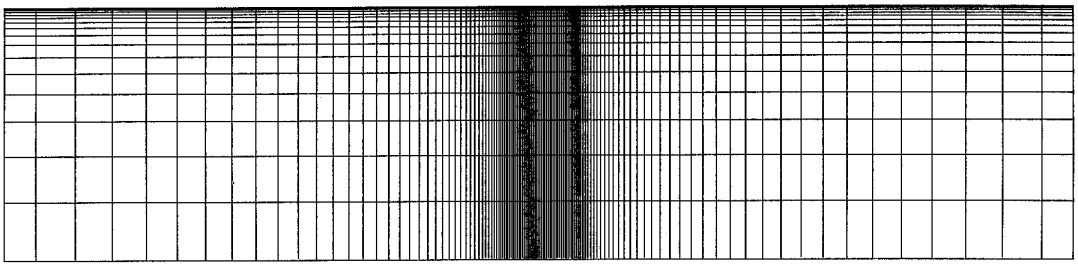

Rapid Prototyping Journal
Volume 4 · Number 1 · 1998 · 26–36

where $[K]$ is the global stiffness matrix, $\{F\}$ is the force vector, $\{\delta\}$ is the displacement vector, and $\{H\}$ is the thermal force vector.

Since neither force nor displacement can be prescribed at the contact surface, moreover contact length cannot be known initially, both force $\{F\}$ and displacement $\{\delta\}$ vectors are unknown. Therefore, equation 21 cannot be directly solved. In order to tackle this problem the iterative procedure described in Sonmez and Hahn (Forthcoming b) is used.

Location of the nip point

Finally, the location of the nip point where the freshly laid sheet and the laminate merge is checked. The exact location depends on the deformed shape of the structure, which is not known at the beginning. Initially a suitable distance, l, between the y axis and the nip point is assumed and the deformed shape is determined by solving equation 21. If the resulting angle between the tape and the laminate, θ, is equal to zero, the distance is considered to be correct (Figure 7a). In this case, normal stress at the nip point also becomes zero. If the angle is less than zero, which is physically not possible, the distance l is smaller than the correct one (Figure 7b). In the case of non zero θ, the location of the nip point is modified and the above calculations are repeated. The iterations are continued until the angle θ becomes zero within an acceptable tolerance. If the angle θ is between 0.0 and 1.0E-2, this requirement is assumed to be met. However, the solution may not be unique. In this case, the correct location of the nip point corresponds to the smallest l that satisfies the zero-angle requirement.

Solution procedure

Figure 8 shows the solution procedure used in the analysis. The thermal and stress analyses are fully coupled. The temperature field generated by the thermal analysis is used in the stress analysis to calculate thermal strains. The contact length under the roller determined by the stress analysis is used as a boundary condition in the thermal analysis. Since the laminate is heated through the contact with a hot roller in the LOM process, accurately determining the contact length is important for the heat transfer analysis. In the stress analysis a different kind of mesh structure is used. For this reason, the temperature field determined by the thermal analysis is mapped to the grid used in the stress analysis by linear interpolation. Besides, the y axis in the stress analysis passes through the center of the roller, whereas in the thermal analysis, it passes through the nip point. The distance between them is l as shown in Figure 7. Every time l changes during the iterations, the thermal analysis is repeated due to the changed boundary condition to calculate the new temperature distribution, which is then remapped. The stress analysis problem is solved again using the new temperature field. This iterative process is continued until θ becomes zero and the difference in temperature field obtained in two consecutive iterations becomes negligibly small.

Figure 7 Determining the location of the nip point; a) *l* corresponds to the exact location of the nip point; b) *l* is too small

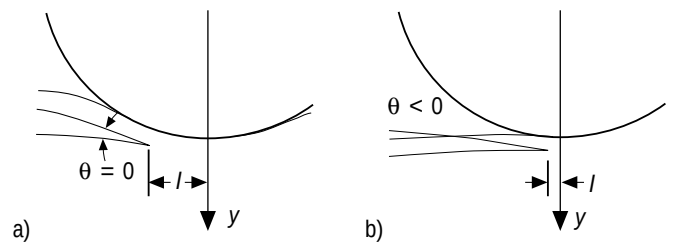

Results and discussions

Verification

Computer codes for stress and heat transfer analyses were developed following the aforementioned solution procedures. The codes were verified by comparing the results with known analytical solutions for similar problems (Sonmez and Hahn; forthcoming a; forthcoming b). The heat transfer model is also verified by comparing the results with the experimental data (Sung Pak (nd)) (see Appendix, Table AI). Figure 9 shows the temperature data points at the top surface of the laminate and the predictions of the present heat transfer analysis. The height and width of the laminate were 2.54cm and 20.32cm, respectively. The roller moved with a constant velocity of 2.54cm/s. The ambient, T_a, and the far field temperature, T_c, were 25°C. An infrared camera was positioned vertically, which started to register the temperature immediately after the roller passed. The temperature profiles predicted by the model are close to the data points.

Figure 8 The solution procedure of the fully coupled thermomechanical problem

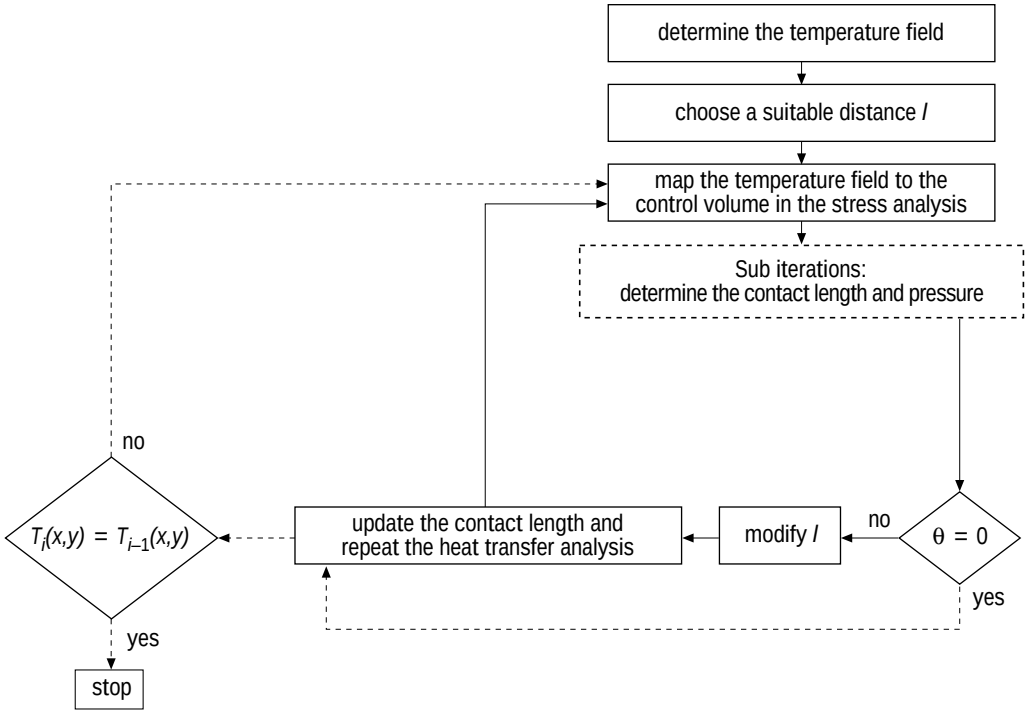

Inputs

Temperature and stress distributions within the laminate were obtained for different sets of process parameters. Most of the data are provided by Helisys (Sung Pak (nd)) and correspond to the actual operation conditions and the materials used. Input parameters for the heat transfer and stress codes are given in Table I and Table II, respectively. Temperature dependent data for thermal expansion coefficient are shown in Figure 10. T_c, T_{room}, and T_a are measured quantities corresponding to the usual operating conditions.

Figure 11 shows the temperature and the normal stress distributions at the interface. The discontinuity in the stress and temperature profiles occurs at the nip point, where the new sheet merges with the previously laid laminate. One could observe that the stress field is more concentrated than the temperature field. Stresses decay to zero values after the roller passes while the temperature at the interface is still above the glass transition temperature of the adhesive. It is advisable to keep the compressive stresses until the material cools below the glass transition point to prevent delamination. This could be achieved by applying a secondary roller right behind the first one. The optimum location of this secondary roller can be determined from the models. As Figure 11 shows, during the contact with the roller, the laminate heats up from medium temperatures to above the glass transition temperature. Considering that bonding could occur only above the glass transition temperature and under compressive stresses, a significant portion of the contact zone, where compressive stresses prevail, does not contribute to bonding. This problem can be remedied, if the laminate is preheated to a temperature close to the glass transition point. In this way, the interface temperature is quickly raised above the glass transition point, and bonding starts immediately after the interface experiences compressive stresses.

The effect of laminate thickness

It should be remembered that nowhere in the analysis has any assumption on the laminate thickness been made. The analysis is applicable to the rolling of a slab of any thickness. Figure 12 shows the stress distribution at the interface for different laminate thicknesses. The roller indentation is the same for all the cases. The smaller the thickness, the higher stresses become. The effect of thickness persists even after the laminate becomes very thick. In order to obtain uniform stress distributions throughout the process, the roller indentation should be increased as the thickness increases. As shown in Figure 13, higher temperatures are obtained for thin laminates due to longer contact lengths.

The effect of roller radius

Figure 14 and Figure 15 show the stress and temperature distributions at the interface for various roller radiuses. As the roller diameter

Rapid Prototyping Journal
Volume 4 · Number 1 · 1998 · 26–36

Figure 9 Temperature data points at the top surface of the laminate and the predictions of the present heat transfer analysis

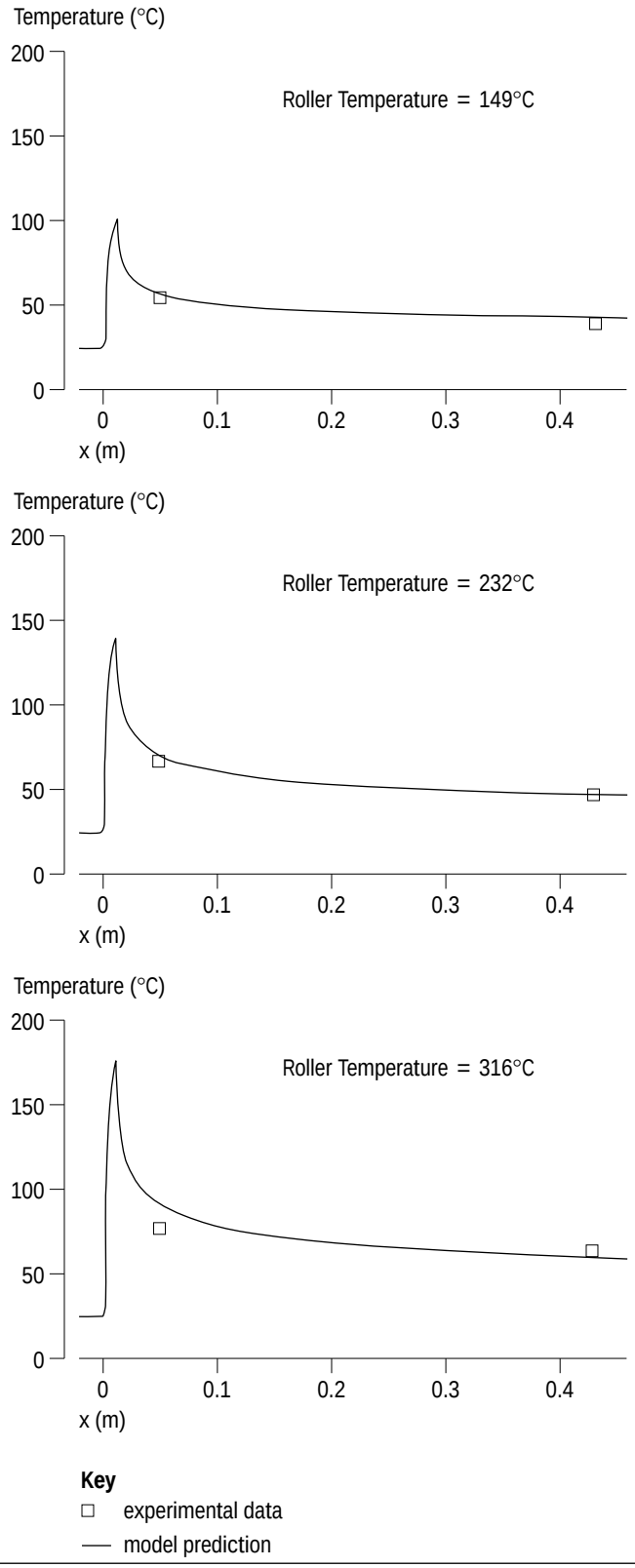

gets smaller, the stresses become higher and more concentrated. Since very high stresses could damage the material, small roller sizes may adversely affect the properties of the final part. If the stress profile under the roller is very concentrated, the time spent under high stresses will also be shorter. This may lead to incomplete bonding and delaminations. Therefore, larger roller diameters are better for consolidation. However, as Figure 15 shows, using larger rollers results in higher temperatures because of longer contact lengths, and thus causes more thermal degradation. Roller temperature should then be reduced for larger diameters.

Table I Input data for the heat transfer analysis

Material property data	
ρ, density	1,449kg/m^3
T_g, glass transition temperature	90°C
k_L, longitudinal conductivity (22°C)	0.2256W/m°C
(90°C)	0.5954W/m°C
k_T, transverse conductivity (22°C)	0.0703W/m°C
(90°C)	0.1784W/m°C
C_p, heat capacity (25°C)	1,455J/kg°C
(50°C)	1,786J/kg°C
Material property data for the mold (aluminum) (Source: Geankoplis, 1983)	
k_b, conductivity (W/m°C)	210
C_b, heat capacity (J/kg°C)	896
ρ_b, density (kg/m^3)	2,707
Geometry of the specimen and the mold (base plate)	
t, thickness of the tape	0.09652mm
number of plies in the substrate	200
y^3, thickness of the mold	1cm
Experiment valuables and boundary conditions	
v_x, roller velocity	2.54cm/s
T_a, ambient temperature	40°C
T_{room}, room temperature	25°C
h_a, heat transfer coefficient of air/laminate interface	20W/m^2°C
h_o, heat transfer coefficient of still air/mold interface	10W/m^2°C
r_1, contact length	5.714mm
r_2, the distance from the nip point to the first contact	0.243mm
T_c, steady-state temperature of the laminate and mold	65°C
T_t, temperature of the new incoming layer (T)	25°C
T_r, temperature of the roller	188°C
h_r, heat transfer coefficient of the roller/ laminate interface	2,300W/m^2°C
Programme variables	
x_1, analyzed length in negative x direction	2cm
x_2, analyzed length in positive x direction	12cm
number of divisions through the length of the strip	184
number of divisions through the thickness of the strip	35

The effect of roller velocity

Figure 16a shows the temperature profiles at the interface for various roller speeds. Roller

Table II Inputs data for the stress analysis

Material properties	
E_1, modulus (in-plane)	9.3GPa
E_2, modulus (transverse plane)	0.814GPa
G_{12}, shear modulus (transverse plane)	0.5GPa
v_{21}, Poisson's ratio (transverse plane)	0.45
v_{21}, Poisson's ratio (in-plane)	0.35
α_{11}, in-plane thermal expansion coefficient (25°C-60°C)	1.31×10^{-5}
α_{22}, transverse thermal expansion coefficient (25°C-60°C)	15.1×10^{-5}
μ, friction coefficient	0.02
Geometry of the specimen	
***t*, thickness of the tape**	0.09652mm
***h*, thickness of the laminate**	19.304mm
***r*, radius of the roller**	5.055cm
Experiment variables	
***d*, indentation of the roller**	0.127mm
***l*, offset between the nip point and center of the roller**	3.1mm
T_o, base temperature for thermal expansion	65°C
Program variables	
length of the strip to be analyzed	2cm
total number of nodes used	2,830
number of divisions through the length of the strip	120
number of divisions through the thickness of the strip	22

Figure 10 Thermal expansion coefficients

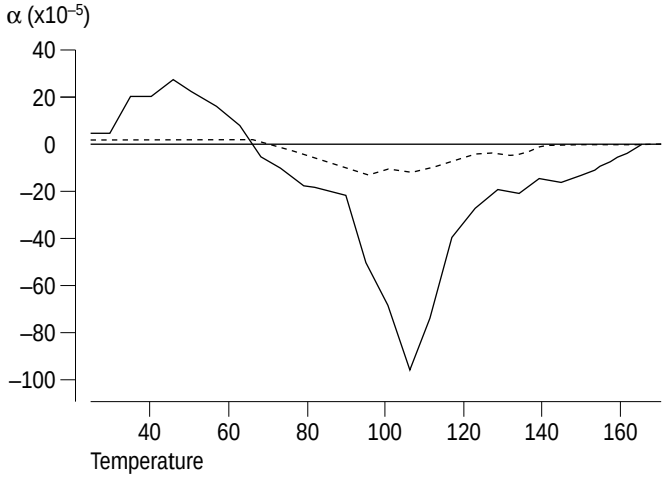

Source: Sung Pak

temperature is modified for each case to keep the maximum temperature within the laminate constant. The maximum temperature occurs at the top surface (Figure 16b).

At high speeds, heat transfer is dominated by heat transport. Only the portions of the laminate that are close to the area in contact with the roller experience high temperatures, and very high temperature gradients exist around the contact surface. For that reason, the temperature at the interface corresponding to the highest roller speed is the lowest, even though temperature states at the top surface are about the same (Figure 16b). At very low speeds, heat transfer is dominated by conduction rather than heat transport. Temperature inside the laminate substantially increases due to heat conduction from the contact surface. Even the temperatures of the

Figure 11 Normal stress and temperature distribution at the interface

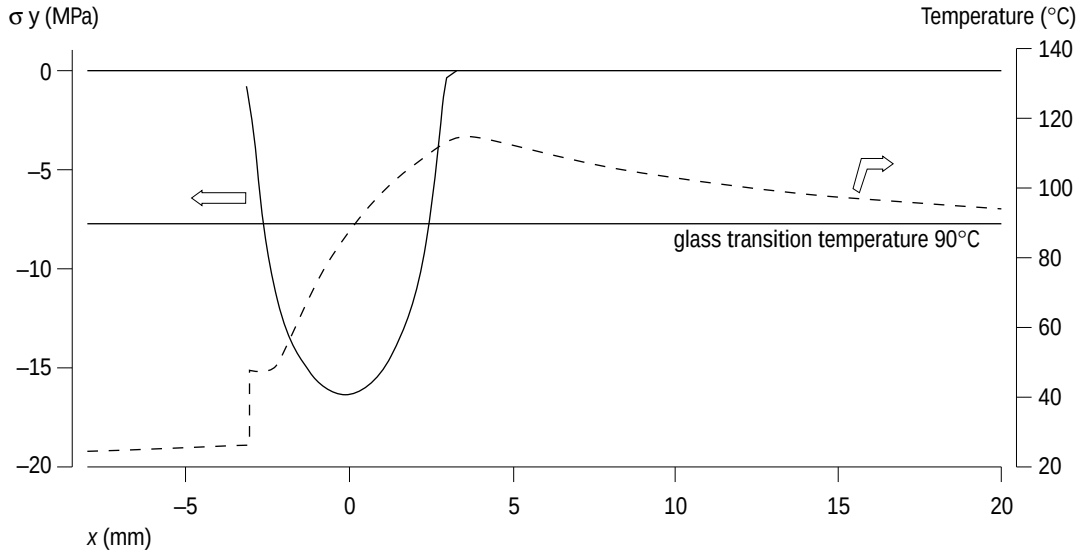

Rapid Prototyping Journal
Volume 4 · Number 1 · 1998 · 26–36

Figure 12 The effect of laminate thickness on the stress distribution at the interface

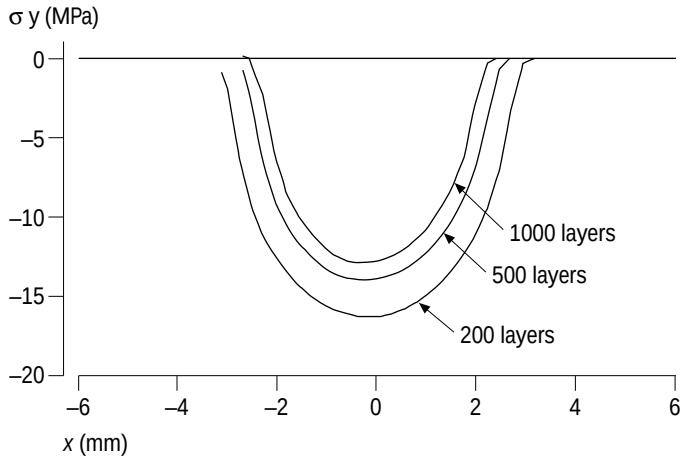

Figure 13 Temperature profiles at the interface for various laminate thicknesses

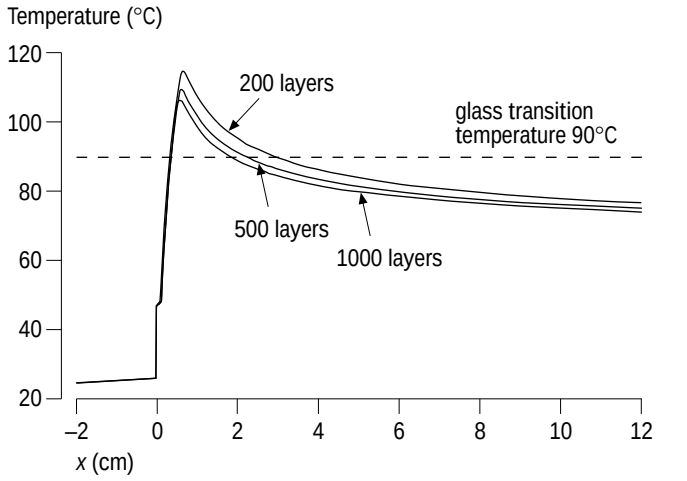

Figure 14 The effect of roller radius on the normal stress distribution at the interface

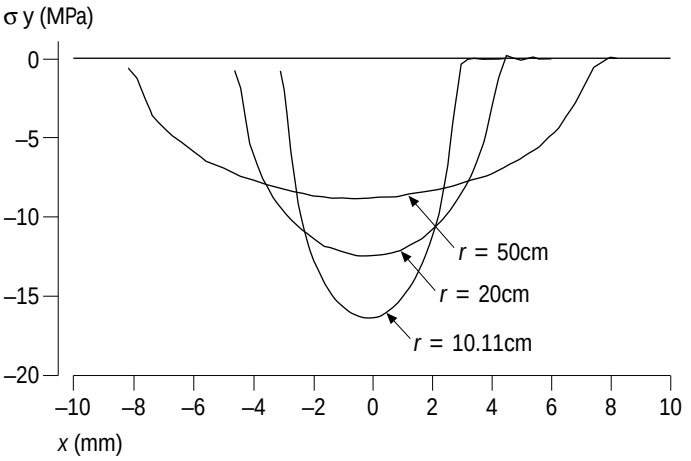

Figure 15 Temperature profiles at the interface for various roller radii

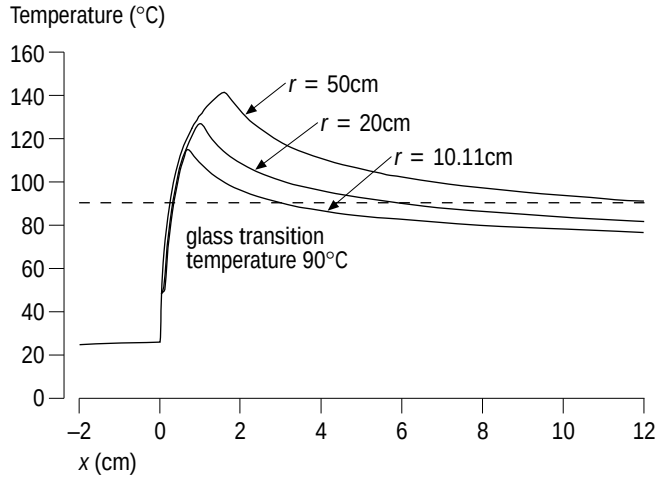

Figure 16 Temperature profiles at the interface (a) and at the top surface (b) for various roller speeds

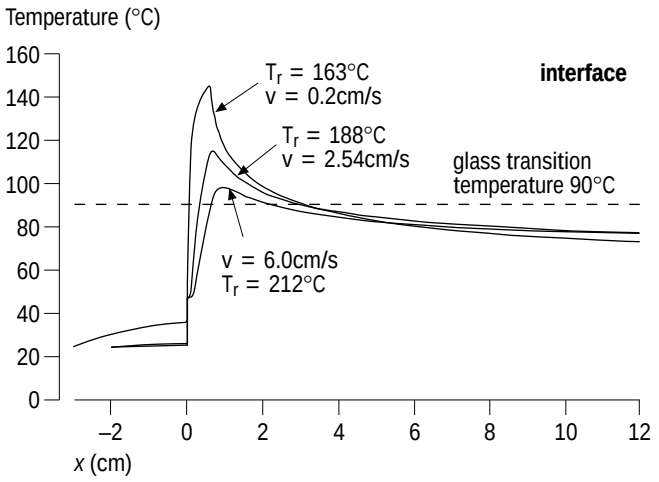

a)

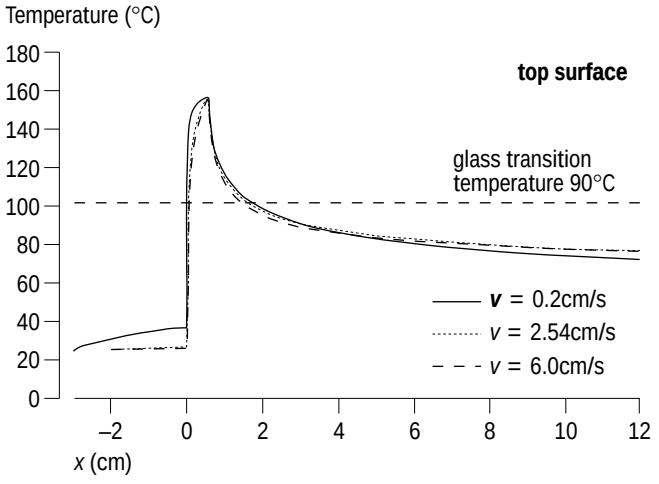

b)

Rapid Prototyping Journal
Volume 4 · Number 1 · 1998 · 26–36

incoming sheet and laminate increase, while at high speeds they remain virtually at room temperature until they enter the heated region.

Conclusions

In this study, stress and heat transfer analyses of the LOM process have been carried out, and the effects of the process parameters on the resulting stress and temperature distributions have been investigated.

Roller-induced normal stresses are quite concentrated at the interface. Stresses decay to zero values while the interface is still above the glass transition temperature of the adhesive. In order to maintain the pressure at the interface until the glass transition temperature is reached, application of a secondary roller or a compaction shoe is advised.

Small rollers induce very concentrated stress distributions at the interface, and thus allow shorter times for bonding. Therefore, large roller diameters are more favorable to bonding.

Thickness of the laminate greatly affects the stress distribution. Higher stresses are induced in thin laminates. By controlling the roller indentation throughout the placement process, uniform stress distributions at ply-interfaces can be obtained.

At high roller speeds, time spent under the roller-induced high stresses is quite short. Bonding in this case may not be complete. Therefore, there is an upper limit for the roller speed above which bonding is not possible.

References

Batra, R.C. (1977), "Cold sheet rolling, the thermoviscoelastic problem. A numerical solution," *International Journal for Numerical Methods in Engineering*, Vol. 11, pp. 671-82.

Brodkey, R.S. and Hershey H.C. (1988), *Transport Phenomena*, McGraw-Hill, New York, NY.

Chua, C.K. (1994), "Three-dimensional rapid prototyping technologies and key development areas," *Computing & Control Engineering Journal*, Vol. 5 No. 4, pp. 200-6.

Feygin, M., Hsieh, B. and Melkanoff, M.A. (1992), "Laminated object manufacturing (LOM): a new tool in the CIM world," *Eighth International PROLAMAT Conference, Man in CIM, Tokyo, Japan, Vol. B-3*, pp. 457-64.

Geankoplis, C.J. (1983), *Transport Processes and Unit Operations*, Allyn & Bacon Inc.

Kochan, A. (1994), "Parangon uses LOM technology to cut product development times," *Assembly Automation,* Vol. 14 No. 2, pp. 32-4.

Lynch, F. de S. (1969), "A finite element method of viscoelastic stress analysis with application to rolling contact problems," *International Journal for Numerical Methods in Engineering*, Vol. 1, pp. 379-94.

Muraski, S.J. (1990), "Make it in a minute (3D plastic model making)," *Machine Design*, Vol. 62 No. 3, February, pp. 127-32.

Pak, S.S. and Nisnevich G. (1994), "Interlaminate strength and processing efficiency improvements in laminated object manufacturing," *Proceedings of 5th International Conference on Rapid Prototyping, Dayton*, pp. 171-80.

Sonmez, F.O. (1995), "Modeling of the thermoplastic composite tape placement process," PhD thesis, UCLA, Los Angeles, CA.

Sonmez, F.O. and Hahn, H.T. (1995), "Simulation of crystallization behavior during thermoplastic tape placement process," *Proceedings of the Tenth International Conference on Composite Materials* (ICCM), Whistler, Canada, August, Part III, pp. 325-32.

Sonmez, F.O. and Hahn, H.T. (forthcoming a), "Process modeling of heat transfer and crystallization for thermoplastic composite tape placement," to appear in *Journal of Thermoplastic Composite Materials.*

Sonmez, F.O. and Hahn, H.T. (forthcoming b), "Thermoviscoelastic analysis of the thermoplastic composite tape placement process," submitted to *Journal of Thermoplastic Composite Materials.*

Sung Pak (nd), Helisys Inc., personal communication.

Wood, L. (1993), *Rapid Automated Prototyping, An Introduction,* Industrial Press Inc., New York, NY.

Yang, T.Y. (1986), *Finite Element Structural Analysis,* Prentice-Hall, Englewood Cliffs, NJ.

Appendix

Table AI Temperature data obtained for three different roller temperatures

Roller surface temperature	149°C	232°C	316°C
Time (min)	Laminate surface temperature (°C)		
0.00	55.0	67.2	72.2
0.25	38.9	46.7	62.8
0.50	36.1	42.8	52.8
0.75	35.0	38.3	–
1.00	33.9	38.3	46.1
2.00	32.2	33.3	40.0
3.00	31.7	32.2	37.8
4.00	30.6	31.1	34.4
5.00	30.0	30.0	34.4

Source: Sung Pak (nd)